

Co-non-solvency: Mean-field polymer theory does not describe polymer collapse transition in a mixture of two competing good solvents

Debashish Mukherji, Carlos M. Marques, Torsten Stuehn, and Kurt Kremer

Citation: *The Journal of Chemical Physics* **142**, 114903 (2015); doi: 10.1063/1.4914870

View online: <http://dx.doi.org/10.1063/1.4914870>

View Table of Contents: <http://scitation.aip.org/content/aip/journal/jcp/142/11?ver=pdfcov>

Published by the [AIP Publishing](#)

Articles you may be interested in

[Density-functional theory for polymer-carbon dioxide mixtures: A perturbed-chain SAFT approach](#)

J. Chem. Phys. **137**, 054902 (2012); 10.1063/1.4742346

[Solvent response of mixed polymer brushes](#)

J. Chem. Phys. **135**, 214901 (2011); 10.1063/1.3657830

[Study of the demixing transition in model athermal mixtures of colloids and flexible self-excluding polymers using the thermodynamic perturbation theory of Wertheim](#)

J. Chem. Phys. **118**, 8525 (2003); 10.1063/1.1565104

[A geometrically-based mean-field theory of polydisperse hard-sphere mixtures](#)

J. Chem. Phys. **107**, 188 (1997); 10.1063/1.474364

[A general mixture theory. II. Mixtures of nonspherical molecules](#)

J. Chem. Phys. **106**, 6116 (1997); 10.1063/1.473233



Co-non-solvency: Mean-field polymer theory does not describe polymer collapse transition in a mixture of two competing good solvents

Debashish Mukherji,¹ Carlos M. Marques,^{1,2} Torsten Stuehn,¹ and Kurt Kremer¹

¹Max-Planck Institut für Polymerforschung, Ackermannweg 10, 55128 Mainz, Germany

²Institut Charles Sadron, Université de Strasbourg, CNRS, Strasbourg, France

(Received 11 December 2014; accepted 2 March 2015; published online 18 March 2015)

Smart polymers are a modern class of polymeric materials that often exhibit unpredictable behavior in mixtures of solvents. One such phenomenon is co-non-solvency. Co-non-solvency occurs when two (perfectly) miscible and competing good solvents, for a given polymer, are mixed together. As a result, the same polymer collapses into a compact globule within intermediate mixing ratios. More interestingly, polymer collapses when the solvent quality remains good and even gets increasingly better by the addition of the better cosolvent. This is a puzzling phenomenon that is driven by strong local concentration fluctuations. Because of the discrete particle based nature of the interactions, Flory-Huggins type mean field arguments become unsuitable. In this work, we extend the analysis of the co-non-solvency effect presented earlier [D. Mukherji *et al.*, Nat. Commun. **5**, 4882 (2014)]. We explain why co-non-solvency is a generic phenomenon, which can only be understood by the thermodynamic treatment of the competitive displacement of (co)solvent components. This competition can result in a polymer collapse upon improvement of the solvent quality. Specific chemical details are not required to understand these complex conformational transitions. Therefore, a broad range of polymers are expected to exhibit similar reentrant coil-globule-coil transitions in competing good solvents. © 2015 AIP Publishing LLC. [<http://dx.doi.org/10.1063/1.4914870>]

I. INTRODUCTION

The microscopic understanding of smart polymer conformations in a mixture of solvents is scientifically challenging¹ and, at the same time, possesses great technological implications that span over a broad range of disciplines.^{2–5} Therefore, establishing the links between smart polymer conformations and its specific interactions is a key to develop any fundamental understanding of their solubility. Examples of the most commonly known smart polymers include: poly(N-isopropylacrylamide) (PNIPAm), poly(N-isopropylmethacrylamide) (PNIPMAm), poly(N,N-diethylacrylamide) (PDEAm), poly(N-vinylcaprolactam) (PVCL), and poly(acryloyl-L-proline methyl ester) (PA-POMe). When some of these polymers are dissolved in a mixture of solvents, such as aqueous alcohol solutions, they show a puzzling coil-globule-coil scenario.^{6–10,14} This interesting phenomenon is termed as co-non-solvency.

Theoretical understanding of these complex phenomena is mostly restricted to a limited number of computer simulation studies,^{1,8,11–14} which usually deal with chemically specific details.^{8,11,12,14,15} Moreover, these simulations require careful parameterization of force fields that can be cumbersome, if there are rather delicate differences in interactions. However, in this context, if a physical phenomenon can be characterized within a universal concept, such that the chemical details only contribute to a pre-factor, then the correct physics can be captured with a rather simple generic model. The use of generic schemes has several advantages; (1) the parameter space is not restricted to a specific system, unlike the all-atom simulations, and a broad range of systems can be

represented within a unified simulation protocol, (2) the time scale of simulations is not of concern, and (3) because of the absence of any competing energy scales, one does not need an advanced molecular dynamics scheme. In this context, we have recently shown that the complexity of smart polymers can be captured within a generic model.¹ Using a simple model, we could quantitatively capture the reentrant coil-globule-coil scenario of PNIPAm^{6–9} and PAPOMe¹⁶ in aqueous methanol mixtures. Our analysis suggested that when two competing and individually good solvents are mixed together, because of the preferential binding of the better of the two (co)solvents with the polymer, it collapses within the intermediate solution compositions. At a low cosolvent concentration, the cosolvent molecules can bind to two distinctly far monomers forming bridges and leading to polymer collapse. When the concentration of the better cosolvent is increased, they decorate the whole polymer and the polymer opens up. These results are in good agreement with the simulations incorporating all-atom details¹⁴ and experiments.⁸ This coil-globule-coil scenario is a generic effect and many polymers are expected to exhibit similar behavior as long as one of the solvents is significantly better than the other. Thus, the behavior is not strictly restricted to the so called smart polymers exhibiting a lower critical solution temperature (LCST). But, also polymers with upper critical solution temperature (UCST) display this behavior, making the co-non-solvency effect independent of their temperature sensitivity. In Table I, we present a list of polymers (both LCST and UCST) that show co-non-solvency effect. It is interesting to note that well known standard polymers, such as poly(ethylene oxide) (PEO) and polystyrene, also show co-no-

TABLE I. A table listing various polymer systems that show co-non-solvency effect when solvated in their respective mixture of solvents.

Polymer (p)	Solvent (s)	Cosolvent (c)
Poly(N-isopropylacrylamide) (PNIPAm) ^{6-9,21}	Water	Methanol, tetrahydrofuran (THF), or 1,4-dioxane
Poly(acryloyl-L-proline methyl ester) (PAPOMe) ¹⁶	Water	Methanol ethanol, or iso-propanol
Poly(ethylene oxide) (PEO) ¹⁷	Water	N,N-dimethylformamide(DMF)
Polystyrene ¹⁸⁻²⁰	Cyclohexane	DMF
Poly(vinyl alcohol) ²²	Water	Dimethyl sulfoxide
Poly(2-(methacryloyloxy)ethylphosphorylcholine) (PMPC) ^{23,24}	Methanol, ethanol, or iso-propanol	Water

solvency.¹⁷⁻²⁰ Note that PEO also exhibits LCST of ~ 373 K.²⁵ Moreover, under ambient conditions, pure water is a good solvent for PEO. Another example may include polymeric semiconductors²⁶ that show anomalous viscosity with solvent composition, suggesting a change in polymer conformation.

One of the most intriguing aspects of the co-non-solvency effect is that the solvent quality becomes increasingly better by the addition of the better cosolvent. Thus, the polymer collapses in a good solvent, making the solvent quality decoupled from the polymer conformation. This is very striking and against the conventional view on polymer solutions. While the atomistic simulations¹⁴ clearly demonstrate that the solvent becomes increasingly better by the addition of better cosolvent, it is still difficult to identify the preferred local coordination and especially the bridging. In contrast, generic simulations give a clear microscopic understanding of this complex phenomenon within a simple simulation protocol.¹

Complementary to that computer simulations give a good microscopic picture of the polymer collapse transitions; it is also advantageous to devise a general analytical theory consistent with the findings known from computer simulations and/or experiments. Moreover, because of the complexity of the system interactions, this discrete particle based phenomenon cannot be explained using a Flory-Huggins type mean-field picture. Instead, these complex conformational transitions can be explained within a Langmuir-like thermodynamic treatment of competitive displacement of different solvent components onto the polymer.¹

In this work, we revisit the co-non-solvency effect of smart polymers in the mixtures of solvents. We extend the analysis of our previous work¹ to better understand the microscopic picture of co-non-solvency. We will present an in-depth argument to show that the mean-field theory is highly unsuitable for these systems and the conceptual need of a discrete particle-based theory. We also propose a phase diagram to identify the conformational states of smart polymers in various bulk solutions and with the change of cosolvent concentrations.

The remainder of the paper is organized as follows: in Sec. II, the generic molecular dynamics simulation details are presented. Results and the theoretical arguments are presented in Sec. III, and we finally present our conclusions in Sec. IV.

II. MODEL AND METHODS

We start by briefly describing the details of the generic molecular simulations. A similar model has been used in our earlier study. A detailed description of model and method

is presented in Ref. 1. Here, a polymer p is modeled using the well known bead-spring polymer model.²⁷ In this model, individual monomers of a polymer interact with each other via a repulsive 6-12 Lennard-Jones (LJ) potential (WCA potential). Additionally, adjacent monomers in a polymer are connected via a finitely extensible nonlinear elastic potential (FENE). Here, $p-p$ interaction energy is chosen as $\epsilon_p = 1.0\epsilon$, and the size of the monomer is $\sigma_p = 1.0\sigma$. All units are expressed in terms of the LJ energy ϵ , the LJ radius σ , and the mass m of individual particles. This leads to a time unit of $\tau = \sigma\sqrt{m/\epsilon}$. The parameters of the potential are such that a reasonably large time step can be chosen, while bond crossing remains essentially forbidden.

A bead-spring polymer is solvated in mixed solutions composed of two components also modeled as LJ beads, solvent s , and cosolvent c , respectively. Since the solvent molecules typically are much smaller than the monomers of PNIPAm and/or PAPOMe in aqueous methanol, we choose the sizes of (co)solvents to be $\sigma_{s/c} = 0.5\sigma$. Note that because of the reduced size of (co)solvents, the corresponding number density within the simulation domain should also be adjusted such that the overall pressure remains $\sim 40\epsilon/\sigma^3$. $p-s$ and $p-c$ interactions are chosen such that c is always a better solvent than s . In our earlier study,¹ the default system consisted of a repulsive $p-s$ interaction, while $p-c$ interaction was attractive. In this work, we generalize this and investigate the effect of asymmetry in interaction energies, when both $p-s$ and $p-c$ are attractive with interactions ϵ_{ps} and ϵ_{pc} , respectively. Additionally, we impose conditions; (1) $\epsilon_{ps} < \epsilon_{pc}$, (2) $0.5 < \epsilon_{ps} < 1.0$, and $0.5 < \epsilon_{pc} < 2.5$. Temperature is set to $T = 0.5\epsilon/\kappa_B$, where κ_B is the Boltzmann constant. This leads to a relative energy scale $\epsilon_{pc} - \epsilon_{ps} \leq 3\kappa_B T$. These values are typically comparable to the interaction energy scale for PNIPAm in aqueous methanol. Solvent particles always repel each other with a repulsive LJ potential, with $\epsilon_{ij} = 1.0\epsilon$. This is a good approximation given that the $p-c$ and $p-s$ interactions are dominant, which will be discussed at a later stage.

The cosolvent mole fraction x_c is varied from 0 (pure s component) to 1 (pure c component). We consider three different polymer chain lengths $N_l = 10, 30$, and 100, solvated in 2.5×10^4 solvent molecules for $N_l = 10$ and $N_l = 30$ and 10×10^4 solvent molecules for $N_l = 100$, respectively. The equations of motion are integrated using a velocity Verlet algorithm with a time step $\delta t = 0.005\tau$ and a damping coefficient $\Gamma = 1.0\tau^{-1}$ for the Langevin thermostat. The initial configurations are equilibrated for typically several $10^5\tau$, depending on the chain length, which is at least an order of

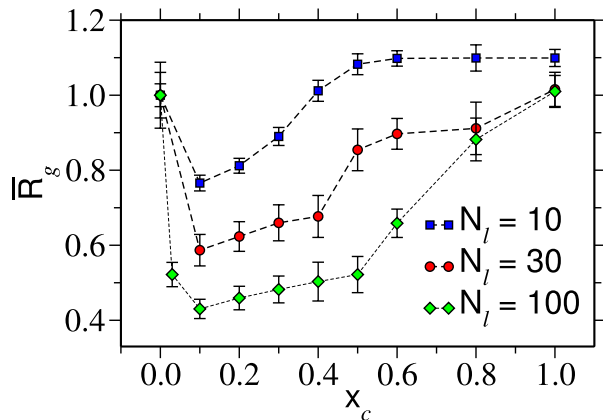


FIG. 1. Normalized radius of gyration $\bar{R}_g = R_g/R_g(x_c = 0)$ as a function of cosolvent molar concentration x_c for three different chain lengths N_l . Results are shown for the default system taken from Ref. 1. The error bars are the standard deviations calculated from six independent simulations. The lines are drawn to guide the eye.

magnitude larger than the relaxation time in the system. After this, initial equilibration averages are taken over another $10^4\tau$ to obtain observables, especially gyration radii R_g , chemical potentials μ_p of the polymer, and the bridging fractions of cosolvents ϕ_B .

III. RESULTS AND DISCUSSIONS

A. Co-non-solvency: A brief overview

In our previous paper,¹ we provided a possible explanation for the experimentally observed co-non-solvency effect of smart polymers in aqueous mixtures.⁶⁻⁹ In Fig. 1, we show the normalized radius of gyration $\bar{R}_g = R_g/R_g(x_c = 0)$ as a function of cosolvent molar fraction x_c . The data are shown for three different N_l . It can be appreciated that just by adding a small fraction of the better of the two solvents, the polymer collapses into a compact globule structure. As discussed in the Introduction, this reentrant collapse and swelling transition is facilitated by the preferential binding of cosolvent components with the polymer. The initial collapse is due to the formation of bridges that the cosolvent molecules form by binding two monomers that can be distinctly far along the backbone of a polymer, while the reopening at higher concentrations is due to the increased decoration of the polymer by cosolvent molecules. Therefore, we can identify two kinds of cosolvents: fraction ϕ_B of bridging cosolvents that bind to two monomers, and a fraction ϕ of cosolvents that are only bound to one monomer. Note that other than ϕ_B and ϕ , there are a large fraction of free cosolvents that are present in the bulk solution and usually are required to maintain solvent equilibrium.

It is also interesting to observe an inverse system size effect in the reopening transition, as observed in Fig. 1. While the initial collapse ($x_c < 0.1$) is reminiscent of a first-order-like collapse, the reopening (for $x_c > 0.5$) is rather smooth even for longer chain lengths. This is contrary to the knowledge of critical phenomena. Thus, indicating that this transition is not a phase transition in a true thermodynamic sense. This aspect will be discussed at a later stage of this

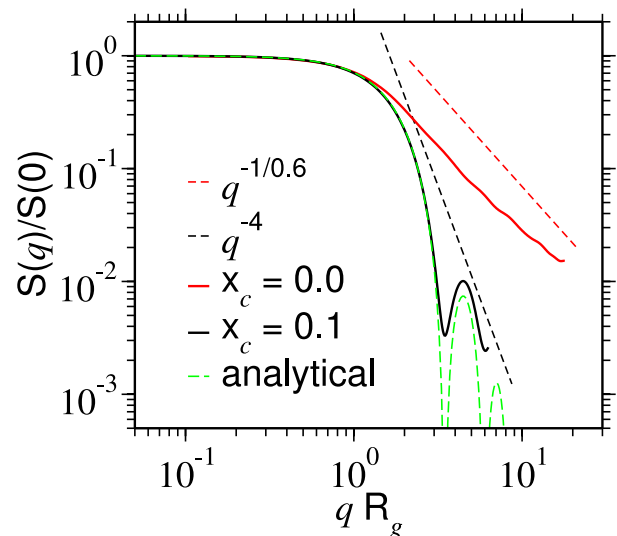


FIG. 2. Static structure factor $S(q)$ for a chain length $N_l = 100$ and for two different mole fractions x_c . A power law of $q^{-1/\nu}$ with $\nu = 0.6$ shows an extended (good solvent) conformation and q^{-4} supports a compact globule structure. For comparison, we have also plotted the analytical scattering function of a sphere.

manuscript. Furthermore, the cosolvent driven first-order-like collapse for $x_c \leq 0.1$ is reminiscent of the temperature induced first order transition in PEO.²⁸

To further quantify the collapse, facilitated by bridging cosolvents, we calculate the static structure factor $S(q)$,^{28,29}

$$S(q) = \frac{1}{N_l} \left\langle \left| \sum_i e^{i\mathbf{q} \cdot \mathbf{R}_i} \right|^2 \right\rangle. \quad (1)$$

In Fig. 2, we present $S(q)$ for $N_l = 100$. As expected, a power law well approximated by $q^{-1/0.6}$ is observed for $x_c = 0$ (pure solvent), a signature characteristic of an extended coil structure. For $x_c = 0.1$, the polymer collapses into a compact globule, with $\sim 60\%$ decrease in R_g with respect to its original extended R_g at $x_c = 0$ (see Fig. 1), as shown by a prominent scaling law q^{-4} in Fig. 2.²⁹ Note that R_g for $x_c = 0.1$ is slightly larger than the equivalent R_g when a polymer collapses because of pure depletion effects. This is due to the fact that a collapsed polymer also contains interstitial bridging cosolvent, and their sizes contribute towards a slightly larger globule.

Preferentiability is required for the observation of the co-non-solvency effect. Therefore, conformations of polymers in mixed solvents are intimately linked to the asymmetry in $p-c$ and $p-s$ interactions $\varepsilon_{pc} - \varepsilon_{ps}$. In Fig. 3, we present a unified picture of polymer conformation with changing $\varepsilon_{pc} - \varepsilon_{ps}$ at different x_c . It can be appreciated that, for $\varepsilon_{ps} = \varepsilon_{pc}$, co-non-solvency is not observed and the polymer remains in a coil conformation. Only when $\varepsilon_{pc} - \varepsilon_{ps} > 0.25\kappa_B T$, does the polymer exhibit a coil-globule-coil-like scenario. More interestingly, the larger the difference $\varepsilon_{pc} - \varepsilon_{ps}$ the smoother the re-opening transition at larger x_c values. This is not surprising given that for a stronger ε_{pc} , ϕ_B has stronger binding, thus leading to a more stable semi-collapsed conformation. Thermodynamically, the energy density in the solvation shell can be increased by increasing the $p-c$ interaction strength. Increasing energy density by a factor

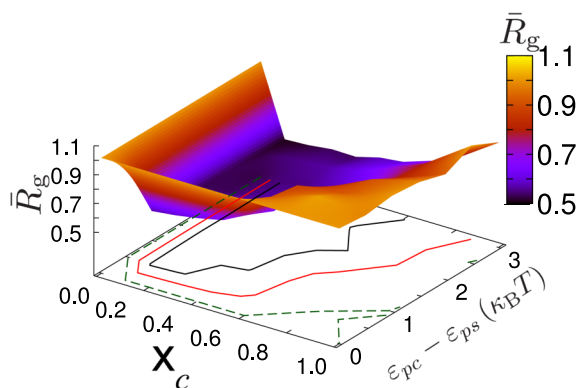


FIG. 3. A sketch of the phase diagram showing the change in normalized radius of gyration $\bar{R}_g = R_g/R_g(x_c=0)$ with the varying cosolvent molar concentration x_c and the relative interaction strengths $\epsilon_{pc} - \epsilon_{ps}$. Results are shown for chain length $N_l = 30$. In the contour plots, the area bound by the black curve represents maximum collapse with $\bar{R}_g < 0.6$. The red contour curve represents the boundary when polymer goes from globule-coil (or vice-versa) by either changing x_c at a constant $\epsilon_{pc} - \epsilon_{ps}$ or by changing $\epsilon_{pc} - \epsilon_{ps}$ at constant x_c . The region outside the dashed green curve shows maximum extension of the chain with $\bar{R}_g \geq 1.0$. Prominent kink in the black contour curve is due to the error bar associated with that data points.

of two will approximately act in a similar manner as that of a polymer of twice N_l . Interestingly enough, increased ϵ_{pc} and/or N_l has the same effect on the overall polymer conformation.

We also want to point out that, for $\epsilon_{pc} \gg \epsilon_{ps}$, polymer collapse will occur close to $x_c \rightarrow 0$. A more prominent representation of the region $0.0 < x_c < 0.1$ will require fine grids and systematic scanning of the concentrations within the range $0 < x_c < 0.1$. Here, however, while the initial collapse is always first order like, the re-opening has much stronger dependence on $\epsilon_{pc} - \epsilon_{ps}$. Therefore, we abstain from presenting any more details within $0 < x_c < 0.1$.

The most interesting aspect of this reentrant transition is that even when the solvent quality becomes better and better by the addition of the better solvent, the polymer collapses in good solvent. This makes the polymer conformation decoupled from the solvent quality and only dictated by the preferential coordination of cosolvent with polymer. This particle based phenomenon cannot be explained within a mean-field type approach.

Before describing an analytical theory, we briefly want to comment on the suitability of the generic simulation protocol to study the complexity of smart polymers. One important aspect of smart polymers, such as PNIPAm, PVCL, and PAPOMe, is their thermal responsiveness. These polymers remain in a coil configuration at low temperatures, while collapsing into a compact globule at high temperatures, thus presenting a LCST. In this context, it is worth mentioning that the generic schemes do not present LCST and co-non-solvency can be studied at one fixed temperature, over full range of x_c . Moreover, the co-non-solvency effect is not necessarily restricted to “so called” smart polymers exhibiting LCST. Therefore, a broad range of polymers are expected to show a similar reentrant scenario, as long as they are dissolved in a mixture of competing good solvents. A list of the possible polymer systems that show co-non-solvency is presented in

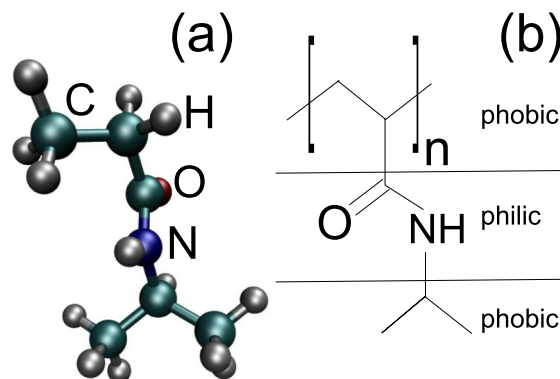


FIG. 4. Part (a) shows simulation snapshot representing a monomer of PNIPAm. Hydrogen atoms is rendered in steel, green spheres are carbon atoms, blue sphere is nitrogen, and the oxygen is rendered in red. Part (b) represents a schematic representation of NIPAm monomer.

Table I. Standard polymers, such as PEO in aqueous DMF¹⁷ and polystyrene in a mixture of N,N-dimethylformamide (DMF) and cyclohexane,^{18–20} also show co-non-solvency. Another example includes polymeric semiconductors. It has been observed that the solution viscosity of polymeric semiconductors can display a non-monotonic dependency of solvent evaporation, pointing to possible conformational changes.²⁶ Therefore, we speculate that many more polymers, such as polycarbonate or polypropylene, may also exhibit a similar reentrant transition in appropriate competing good solvents. Although we have not performed any analysis based on the temperature effects on the chain collapse, we anticipate that the UCST associated with the generic model will increase in the full range of x_c . On the other hand, LCST behavior, in principle, can be reproduced using a temperature dependent interaction parameters that can incorporate hydrogen bonding within a simplified model.

Another aspect is that the NIPAm monomer has a hydrophilic part and two hydrophobic parts, as shown in the schematic Fig. 4. It is generally believed that methanol molecules bind to the hydrophilic part and thus push away water molecules towards the hydrophobic part, leading to polymer collapse. In a generic simulation, however, the monomer is represented by a sphere, thus eliminating any effects due to hydro(phob/philicity) within the model. Our simulations^{1,14} suggests that the only dominant interaction is the preferential coordination of methanol around the NIPAm monomer (see Fig. 3 of Ref. 14). The collapse is initiated by bridging and not by any hydrophobic effects that may occur due to solvent interaction with the alkane backbone. Chemical details do not play any role in describing this reentrant transition. In this context, tuning specific (co)solvent-polymer interactions, a whole new class of heteropolymers can also exhibit co-non-solvency and related phenomena.³⁰

B. Co-non-solvency: A simple analytical approach

1. Why mean-field theory is inappropriate to describe co-non-solvency

When a polymer with chain length N_l at volume fraction ϕ_p is dissolved in a mixture of two components s and

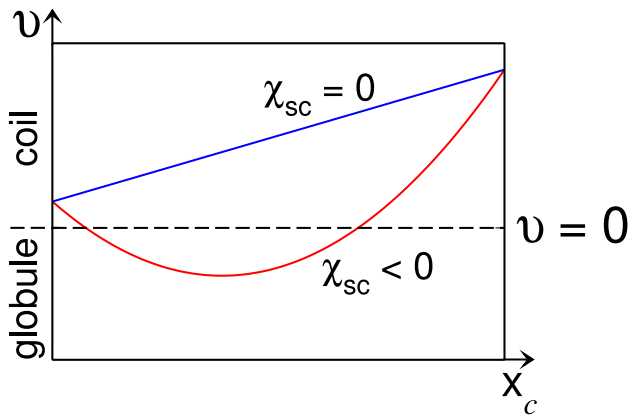


FIG. 5. A schematic representation of the polymer excluded volume v as a function of cosolvent mole fraction x_c . The curve shows that the interaction parameter χ_{sc} between solvent-cosolvent is a key factor to exhibit a swelling-collapse-swelling scenario. When $\chi_{sc} = 0$, the polymer remains swollen.

c , respectively, the standard Flory-Huggins energy \mathcal{F}_{FH} of polymer solutions reads^{31,32}

$$\begin{aligned} \frac{\mathcal{F}_{\text{FH}}}{\kappa_B T} = & \frac{\phi_p}{N_l} \ln \phi_p + x_c (1 - \phi_p) \ln [x_c (1 - \phi_p)] \\ & + (1 - x_c)(1 - \phi_p) \ln [(1 - x_c)(1 - \phi_p)] \\ & + \chi_{ps} \phi_p (1 - x_c)(1 - \phi_p) + \chi_{pc} \phi_p x_c (1 - \phi_p) \\ & + \chi_{sc} x_c (1 - x_c)(1 - \phi_p)^2. \end{aligned} \quad (2)$$

Here, the first three terms represent the entropy of mixing and the last three terms deal with interactions between different components i and j via χ_{ij} . Expanding Eq. (2) to the second order gives a direct measure of the excluded volume \mathcal{V} of the polymer,^{31,32}

$$\mathcal{V} = 1 - 2(1 - x_c)\chi_{ps} - 2x_c\chi_{pc} + 2x_c(1 - x_c)\chi_{sc}, \quad (3)$$

where χ_{ps} and χ_{pc} are the Flory-Huggins interaction parameters between $p-s$ and $p-c$, respectively. The factor χ_{sc} is the parameter of $s-c$ interaction. When both solvent and cosolvent are good solvents, $\chi_{ps} < 1/2$ and $\chi_{pc} < 1/2$.⁶ Using the first two terms of Eq. (3), we find a linear variation of \mathcal{V} with x_c for the cases of non-interacting s and c (i.e., $\chi_{sc} = 0$), as shown by the blue line in Fig. 5. It is also clear from Fig. 5 that only when $\chi_{sc} < 0$, \mathcal{V} can become negative, opening the possibility for the coil-to-globule-to-coil conformation changes typical of co-non-solvency. It has been noticed early⁶ that for common solvent mixtures where co-non-solvency effects are observed, such as water-alcohol mixtures, $\chi_{sc} > 0$, thus precluding any explanation based on a mean-field, Flory-Huggins type of analysis.

Furthermore, within the mean-field picture described in Eq. (2), one can get the expression for the shift in chemical potential of polymer $\bar{\mu}_p$ for $\phi_p \rightarrow 0$,

$$\begin{aligned} \bar{\mu}_p(\phi_p \rightarrow 0) = & \left. \frac{\partial \mathcal{F}_{\text{FH}}}{\partial \phi_p} \right|_{\phi_p \rightarrow 0} \\ = & \text{const} - x_c \ln x_c - (1 - x_c) \ln(1 - x_c) \\ & + (1 - x_c)\chi_{ps} + x_c\chi_{pc} - 2x_c(1 - x_c)\chi_{sc}. \end{aligned} \quad (4)$$

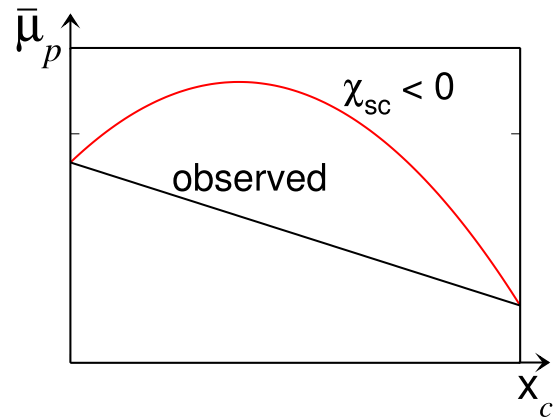


FIG. 6. A schematic representation of the shift in chemical potential $\bar{\mu}_p$ as a function of cosolvent mole fraction x_c .

In Fig. 6, we present a schematic representation of $\bar{\mu}_p$ as expected from Flory-Huggins picture described in Eq. (4). Here, $\bar{\mu}_p(x_c = 1) < \bar{\mu}_p(x_c = 0)$ because alcohol is a better solvent compared to water. Consistently with the behavior of \mathcal{V} presented in Fig. 5, $\bar{\mu}_p$ for $\chi_{sc} < 0$ displays a hump for intermediate mixing ratios where the solvent quality goes from good to poor to good again (see red curve in Fig. 6). However, in our simulations,^{1,14} not only is $\chi_{sc} = 0$, but we also measure a chemical potential trend similar to the black schematic curve in Fig. 6. Thus, the solvent quality remains good in the whole composition range, and, in-fact, it even becomes increasingly better by the addition of the cosolvent. By the analysis of Eq. (4), it can be seen that a similar trend as the black curve of Fig. 6 can be obtained from the mean-field picture when $\chi_{sc} \gg 0$. However, this can only be obtained at the nonrealistic cost of driving the system towards solvent phase separation. This further confirms the incapability of mean-field theory to capture the reentrant co-non-solvency effect in polymeric systems.

The mean-field picture also suggests that the strength of $s-c$ interaction should be dominant over $p-s$ and $p-c$ interactions to observe this reentrant transition. Moreover, if the mean-field theory is sufficient to understand this reentrant coil-globule-coil transition then the analysis of the bulk solution property, that can easily be calculated using molecular simulations, should also show a preferred $s-c$ coordination over $p-s$ or $p-c$ coordination.

A quantity that best describes the relative intermolecular affinity and/or the interaction strength is the fluctuation theory of Kirkwood and Buff (KB).³³ KB theory connects the pair distribution function to thermodynamic properties of solutions using the “so called” KB integrals,

$$G_{ij} = 4\pi \int_0^\infty [g_{ij}(r) - 1] r^2 dr, \quad (5)$$

where $g_{ij}(r)$ is the pair distribution function. In Fig. 7, we summarize G_{ij} between different solvent components. It can be appreciated that, for $0.1 < x_c < 0.5$, $p-c$ coordination is at-least an order of magnitude larger than the G_{ij} values between the solvent components in the bulk solution, suggesting that the fraction of cosolvent molecules in close contact with the chain is always much larger than its natural, mean-field

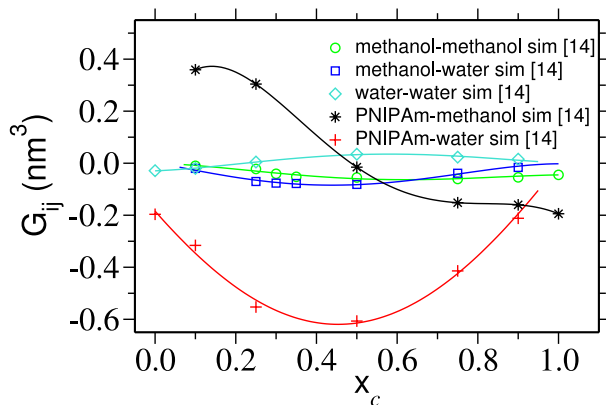


FIG. 7. Kirkwood-Buff integral G_{ij} between different solution components as a function of cosolvent molar fraction x_c . Lines are the polynomial fits to the data that are drawn to guide the eye. The data were obtained from the semi-grand canonical simulations incorporating all-atom details.¹⁴ For pure solvent at $x_c = 0.0$ and pure cosolvent at $x_c = 1.0$, individual coordinations G_{pc} and G_{ps} are undefined, respectively.

proportions in the bulk solution. This is contrary to what is known from the analysis based on the mean-field theory presented above. Furthermore, the shift in chemical potential $\bar{\mu}$ can be estimated from the KB theory. If a polymer p at dilute concentration is solvated in a mixture of solvent s and cosolvent c , μ_p can be calculated using³⁴

$$\left(\frac{\partial \bar{\mu}_p}{\partial \rho_c}\right)_{p,T} = \frac{G_{ps} - G_{pc}}{1 - \rho_c(G_{cs} - G_{cc})}, \quad (6)$$

where $\bar{\mu}_p = \mu_p / \kappa_B T$ and ρ_c is the cosolvent number density. The change in $\bar{\mu}_p$ is shown in Fig. 8. Data clearly show the trend known for the case when $\chi_{sc} = 0$, suggesting that the solvent quality becomes better and better by the addition of better (co)solvent. This decoupling between solvent quality and the polymer conformation is contrary to the conventional understanding from mean-field predictions. Additionally, this conformational transition of polymer in mixtures of competing good solvents is not a phase transition in true thermodynamics sense and is only dictated by the preferential adsorption of one of the (co)solvents. Therefore, an analytical description is needed that can incorporate the concept of competitive adsorption by taking into account the strong deviations of local concentration from mean-field values. We will address this in Sec. III B 2.

2. Competitive adsorption of the cosolvent as a model for co-non-solvency

We have recently proposed that the polymer collapse in co-non-solvency phenomena can simply be understood as the result of the attractive interactions induced by cosolvent molecules that form a bridge between two monomers.¹ Conformational collapse, at low x_c , is thus induced by the increase of such bridges, while polymer swelling at larger cosolvent fractions is due to the progressive replacement of these bridges by single site cosolvent molecules that are attached to one monomer only. Thus, for high enough x_c , these non-bridging cosolvent molecules eventually decorate the whole chain backbone to facilitate the reopening. In Fig. 9, we show ϕ_B , the

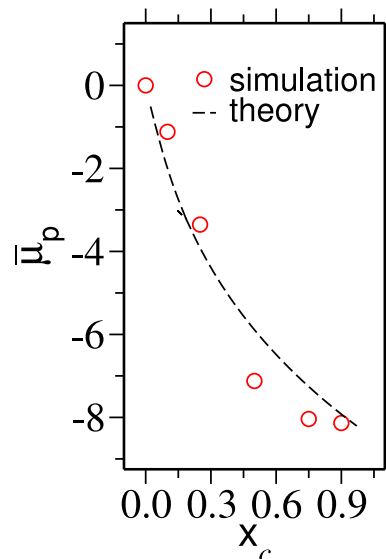


FIG. 8. Shift in chemical potential of a single monomer $\bar{\mu}_p$ as a function of methanol mole fraction x_c . $\bar{\mu}_p$ is calculated by integrating the Eq. (6). G_{ij} are taken from Fig. 7. Dashed line is plotted according to the Eq. (13).

fraction of backbone sites participating in bridge formation, as a function of x_c . Note that ϕ and ϕ_B are cosolvent molecules that are directly in contact with the monomers at a distance $2^{1/6}\sigma_{pc} \sim 0.84\sigma$. It can be appreciated that, within the range $0.1 < x_c < 0.4$, ϕ_B obtained from the numerical simulations shows a distinct hump that is consistent with the range of x_c when the polymer collapses into a (compact) globule and then gradually begins to expand. To devise a theoretical formulation, we view the polymer as a substrate with N sites exposed to the bulk solution, of which n^s sites are occupied by s (solvent) molecules, n^c sites by non-bridging c (co-solvent) molecules, and $2n_B^c$ sites by bridging c (co-solvent) molecules, with $N = n^s + n^c + 2n_B^c$. The observed sequence of collapse and re-swelling of the polymer correspond to a fast growth of

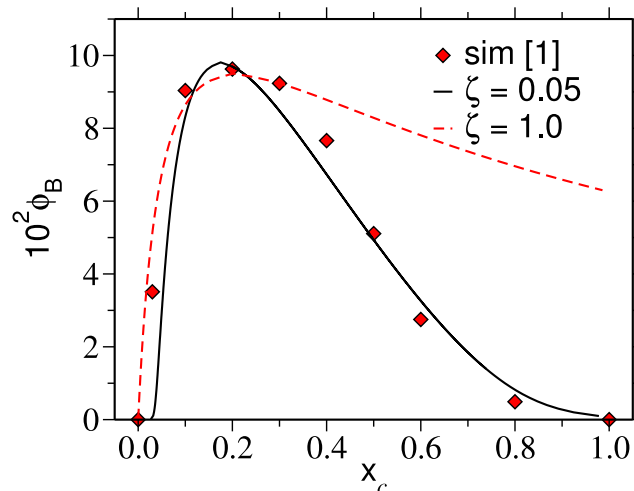


FIG. 9. Bridging fraction of cosolvents ϕ_B as a function of cosolvent mole fraction x_c for $N_l = 100$. The data corresponding to red diamond are the direct calculation of ϕ_B from the simulation trajectory. The prediction of analytical theory from Eq. (8) is plotted for two different ζ parameters. Here $\zeta = 0.05$ corresponds to the translational entropic term corrected with a loop contribution, as observed earlier.¹

n_B^c as x_c increases, followed by a displacement of n_B^c by n^c for larger x_c values. Such a sequence is typical for competitive displacement in adsorption phenomena.³⁵ Our results from numerical simulations for n_B^c and n^c , or alternatively for the fractions $\phi_B = n_B^c/N$ and $\phi = n^c/N$, are very well described by a competitive adsorption model with the following associated free energy density of adsorption for non-bridges and bridges:

$$\begin{aligned} \frac{\Psi}{\kappa_B T} = & \phi \ln(\phi) + \zeta \phi_B \ln(2\phi_B) \\ & + (1 - \phi - 2\phi_B) \ln(1 - \phi - 2\phi_B) \\ & - \mathcal{E}\phi - \mathcal{E}_B \phi_B - \frac{\mu}{\kappa_B T} (\phi + \phi_B), \end{aligned} \quad (7)$$

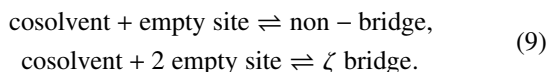
with $\mu = \kappa_B T \ln(x_c)$ being the chemical potential of the cosolvent in the bulk solvent mixture and the adsorption energies \mathcal{E} and \mathcal{E}_B measure the excess affinities of individual non-bridging and bridging cosolvent molecules to the chain monomers. The first three terms in Eq. (7) express entropic contributions of the adsorbed bridges and non-bridges to the energy densities, while the two following terms measure contact energies between the cosolvents bridges and non-bridges with the polymer backbone. The unusual pre-factor ζ is, as discussed later, a consequence of assuming a logarithmic form for the dependence of the energy required to make a bridge on the average density of existing bridges. This is the case, for instance,¹ if one assumes that in order to make a new bridge at density ϕ_B , the chain needs to make a loop of length $\ell = 1/\phi_B$, with associated penalty $\sim \log \ell \sim \log(1/\phi_B)$.

Minimization of Eq. (7) with respect to ϕ_B and ϕ leads to the implicit equation for the bridge density $\phi_B(x_c)$,

$$\begin{aligned} 16\phi_B^\zeta x_c = x_c^* \left\{ \left(\frac{x_c^*}{x_c^{**}} \right)^{1/2} (1 - 2\phi_B) \right. \\ \left. \pm \sqrt{\left(\frac{x_c^*}{x_c^{**}} \right)^2 (1 - 2\phi_B)^2 - 16\phi_B^\zeta} \right\}, \end{aligned} \quad (8)$$

with $x_c^* = \exp(-\mathcal{E})$ and $x_c^{**} = \exp(-\mathcal{E}_B + 2 \ln 2e - \zeta)$ are the characteristic concentrations related to the adsorption energies \mathcal{E} and \mathcal{E}_B for non-bridges and bridges, respectively. Fig. 9 shows that this expression describes very well our simulation results, with $\zeta = 0.05$.

Equation (8) can equivalently be derived by considering the two pseudo-chemical reactions,



A schematic representation of this reaction is presented in Fig. 10. When the solvent and cosolvent interactions with the polymer backbone empty sites are described as pseudo-reactions, a cosolvent molecule reacts with one empty adsorption site to form one adsorbed non-bridge, while it reacts with two empty sites to make ζ bridges. The associated equilibrium standard mass-action laws can thus be

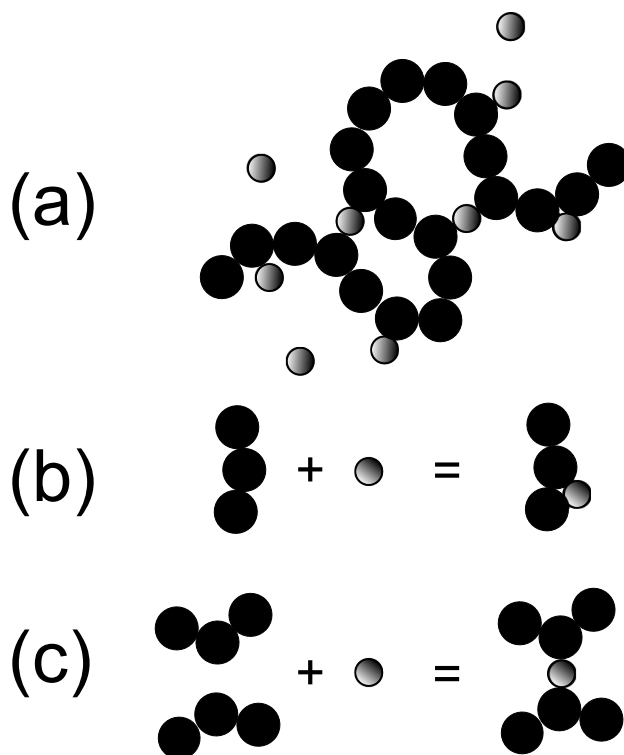


FIG. 10. A schematic representation of the chemical reaction described in Eq. (9). Part (a) describes a typical polymer conformation decorated by non-bridging and bridging cosolvent molecules. While part (b) shows that a polymer segment and a cosolvent forms a single adsorbed non-bridging cosolvent, part (c) represents two segments and a cosolvent makes a bridge (or a bridging cosolvent).

written as

$$\begin{aligned} \frac{x_c}{x_c^*} &= \frac{\phi}{1 - \phi - 2\phi_B}, \\ \frac{x_c}{4x_c^{**}} &= \frac{\phi_B^\zeta}{(1 - \phi - 2\phi_B)^2}, \end{aligned} \quad (10)$$

with equilibrium reaction constants $1/x_c^*$ and $1/x_c^{**}$. Note that the reaction equilibrium concentration x_c^{**} has been, for mathematical convenience, defined up to a factor four. Solving the mass-action laws for ϕ_B gives Eq. (8). In this pseudo-chemical language, the factor ζ describing the effective number of bridges formed by the interaction between one cosolvent molecule and the two empty sites of the backbone appears as a consequence of assuming a power-law dependence for the equilibrium constant of the pseudo-chemical reaction. Note that the actual shape of Eq. (8) is quite sensitive to the value of ζ . In particular, the choice $\zeta = 1$, corresponding to a standard chemical reaction between free species in solution, leads to a prediction that cannot describe our data (see red curve in Fig. 9).

In a previous work,¹ we argued that a value of $\zeta = 0.05$ can be understood by considering loop contributions to the cost of making a bridge. When a pure configurational cost for distributing the bridges amongst the possible occupation sites is combined with the entropic cost of loop formation, one can write $\zeta = 2 - m$. Here, the critical exponent m can be estimated within a simple scaling argument. In this context, one can characterize the loop formation by a partition function

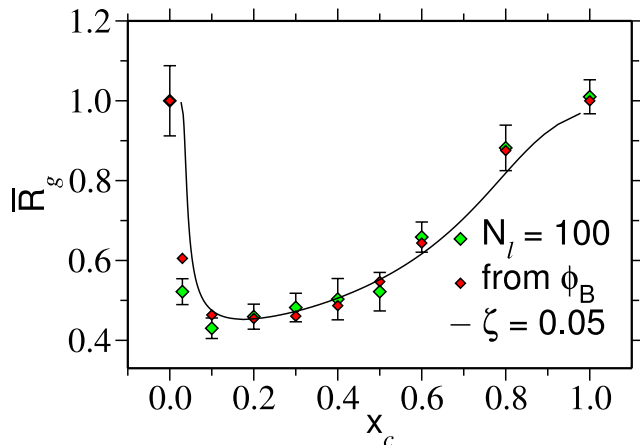


FIG. 11. A comparative plot of the normalized radius of gyration $\bar{R}_g = R_g / R_g(x_c=0)$ as a function of cosolvent molar concentration x_c for a chain length $N_l = 100$. Three legends represent the direct calculation of \bar{R}_g (green diamond symbol), \bar{R}_g calculated from $\phi_B(x_c)$ in Fig. 9 (red diamond symbol), and solid line represents theoretical prediction in Eq. (14).

of vanishing end-to-end distance $R_e \rightarrow 0$,³²

$$Z_{N_l}(R_e \rightarrow 0) \propto q^{N_l} N_l^{\alpha-2}, \quad (11)$$

and the partition function at finite R_e is given by

$$Z_{N_l}(R_e) \propto q^{N_l} N_l^{\gamma-1}. \quad (12)$$

Here, $1/q$ is the critical fugacity and the universal exponent $\alpha \cong 0.2$.³² From these two cases, one can estimate the free energy barrier to form a loop of length ℓ as $\Delta\mathcal{F}(\ell) = m\kappa_B T \ln(\ell)$, with $m = \gamma - \alpha + 1$ being the critical exponent.³² Although this gives $m = 1.95$ for loop formation in self-avoiding walks, in excellent agreement with our findings, it is worth pointing to the fact that our simple analytical description does not address other possible contributions to bridge formation, such as cooperative or other non-trivial entropic effects that might be determinant in the dense chain globule. Note that, consistent with the data from numerical simulations, we do not account for any change of chain rigidity due to competitive solvent displacement.

This selective adsorption model also provides for an analytical prediction of the shift in the chemical potential μ_p as a function of x_c ,

$$\frac{\mu_p}{\kappa_B T} = \text{const} + (2 - \zeta) \phi_B - \ln \left\{ 1 + \phi_B^{1-\zeta/2} \left(\frac{x_c}{x_c^{**}} \right)^{1/2} + \left(\frac{x_c}{x_c^{**}} \right) \right\}. \quad (13)$$

Fig. 8 shows a comparison between predictions from Eq. (13) and the values of the chemical potential obtained from Eq. (6). A very good agreement is obtained by simply inserting into Eq. (13) the values for ζ and concentrations obtained from the fit of the bridging fraction, further confirming the consistency and validity of our approach.

3. Estimation of polymer gyration radii

The process of collapsing a polymer chain from the fully swollen athermal state to a compact globule is well

understood.^{18,31,32} Starting from the swollen state, an increase of the attraction between the monomers first brings the polymer into Θ -conditions, where $R_g \sim N_l^{1/2}$. Further increase of the attraction then collapses the polymer into a globular state. The dimensions of the collapsed globule can be understood by balancing the second virial osmotic contributions with attractive coefficient $-|\mathcal{V}|$ and three body repulsions. This leads to $R_g \sim [N_l/\mathcal{V}]^{1/3}$. In this regime, a simple formula that interpolates between Θ -conditions and the collapsed state can be written as $(R_\Theta/R_g)^3 - 1 \propto \mathcal{V}$. In our case, however, most of the significant behavior occurs when the polymer is collapsed and the interpolation formula,

$$\left[\frac{R_g}{R_g(x_c=0)} \right]^{-3} - 1 = \mathcal{V}, \quad (14)$$

describes very well the chain R_g with x_c over the full composition range when $\mathcal{V} = 100\phi_B(x_c)$, see Fig. 11 build from the corresponding variation of the bridge fraction $\phi_B(x_c)$ in Fig. 9. It is important to note that even when we only show results for $N_l = 100$, the shorter chain length of $N_l = 30$ also displays the similar behavior consistent with $\mathcal{V} = 30\phi_B(x_c)$, thus suggesting that, in general, $\mathcal{V} \simeq N_l\phi_B(x_c)$.

IV. CONCLUSION

We present a comprehensive analysis of the co-non-solvency effect of smart polymers in a mixture of good solvents. Our results suggest that co-non-solvency is a generic effect that is not restricted to any specific chemical systems. While the co-non-solvency has been traditionally associated with smart polymers exhibiting LCST like PNIPAm, PVCL, and/or PAPOMe,^{1,6-8,10,16} standard polymers, such as PEO, poly(vinyl alcohol), and polystyrene, also exhibit co-non-solvency.^{17,20,22} Therefore, polymers presenting UCST also display co-non-solvency, suggesting that the temperature sensitivity of a particular polymer does not play a critical role in describing its conformation in mixtures of two competing good solvents. Furthermore, this reentrant transition is dictated by the preferential coordination of one of the cosolvents with the polymers. More interestingly, even when the chain collapses, the solvent quality becomes increasingly better. This makes the solvent quality disconnected from the conformation of the macromolecules. This discrete particle-based phenomenon cannot be explained within a mean-field theory. Instead, it can be explained using a thermodynamic treatment of a simple selective adsorption picture, where the preferential interaction with the chain includes both, enthalpic contributions and entropic conformational effects. Therefore, this work presents a unified theoretical and computational framework, which can pave the way for a more generic understanding of polymeric solubility in mixtures of solvents.

ACKNOWLEDGMENTS

We thank Alexander Grosberg, Jean-François Joanny, Guojie Zhang, and Kostas Daoulas for many stimulating discussions and Jörg Stellbrink for bringing Ref. 17 to our attention. C.M.M. acknowledges Max-Planck Institut

für Polymerforschung for hospitality where this work was performed. We thank Aoife Fogarty, Robinson Cortes-Huerta, and Debarati Chatterjee for critical reading of the manuscript. Simulations are performed using ESPResSo++ molecular dynamics package,³⁶ and one snapshot in this manuscript is rendered using VMD.³⁷

- ¹D. Mukherji, C. M. Marques, and K. Kremer, *Nat. Commun.* **5**, 4882 (2014).
- ²M. A. Cohen-Stuart, W. T. S. Huck, J. Genzer, M. Müller, C. Ober, M. Stamm, G. B. Sukhorukov, I. Szleifer, V. V. Tsukruk, M. Urban, F. Winnik, S. Zauscher, I. Luzinov, and S. Minko, *Nat. Mater.* **9**, 101 (2010).
- ³M. A. Ward and T. K. Georgiou, *Polymers* **3**, 1215 (2011).
- ⁴S. de Beer, E. Kutnyansky, P. M. Schön, G. J. Vancso, and M. H. Müser, *Nat. Commun.* **5**, 3781 (2014).
- ⁵S. de Beer and M. H. Müser, *Macromolecules* **47**, 7666 (2014).
- ⁶H. G. Schild, M. Muthukumar, and D. A. Tirrell, *Macromolecules* **24**, 948 (1991).
- ⁷G. Zhang and C. Wu, *Phys. Rev. Lett.* **86**, 822 (2001).
- ⁸J. Walter, J. Sehr, J. Vrabec, and H. Hasse, *J. Phys. Chem. B* **116**, 5251 (2012).
- ⁹H. Kojima, F. Tanaka, C. Scherzinger, and W. Richtering, *J. Polym. Sci., Part B: Polym. Phys.* **51**, 1100 (2012).
- ¹⁰F. Tanaka, T. Koga, and F. M. Winnik, *Phys. Rev. Lett.* **101**, 028302 (2008).
- ¹¹J. Walter, V. Ermatchkov, J. Vrabec, and H. Hasse, *Fluid Phase Equilib.* **296**, 164 (2010).
- ¹²A. K. Tucker and M. J. Stevens, *Macromolecules* **45**, 6697 (2012).
- ¹³J. Heyda, A. Muzdalo, and J. Dzubiella, *Macromolecules* **46**, 1231 (2013).
- ¹⁴D. Mukherji and K. Kremer, *Macromolecules* **46**, 9158 (2013).
- ¹⁵F. Rodriguez-Roperio and N. F. A. van der Vegt, *J. Phys. Chem. B* **118**, 7327 (2014).
- ¹⁶A. Hiroki, Y. Maekawa, M. Yoshida, K. Kubota, and R. Katakai, *Polymer* **42**, 1863 (2001).
- ¹⁷R. Lund, L. Willner, J. Stellbrink, A. Radulescu, and D. Richter, *Macromolecules* **37**, 9984 (2004).
- ¹⁸A. R. Shultz and P. J. Flory, *J. Polym. Sci.* **15**, 231 (1955).
- ¹⁹B. E. Read, *Trans. Faraday Soc.* **56**, 382 (1960).
- ²⁰B. A. Wolf and M. M. Willms, *Makromol. Chem.* **179**, 2265 (1978).
- ²¹F. M. Winnik, H. Ringsdorf, and J. Venzmer, *Macromolecules* **23**, 2415 (1990).
- ²²M. Ohkura, T. Kanaya, and K. Kaji, *Polymer* **33**, 3686 (1992).
- ²³Y. Kiritoshi and K. Ishihara, *J. Biomater. Sci., Polym. Ed.* **13**, 213 (2002).
- ²⁴Y. Kiritoshi and K. Ishihara, *Sci. Technol. Adv. Mater.* **4**, 93 (2003).
- ²⁵H. N. Lee and T. P. Lodge, *J. Phys. Chem. Lett.* **1**, 1962 (2010).
- ²⁶G. Hernandez-Sosa, N. Bornemann, I. Ringle, M. Agari, E. Dörsam, N. Mechau, and U. Lemmer, *Adv. Funct. Mater.* **23**, 3164 (2013).
- ²⁷K. Kremer and G. S. Grest, *J. Chem. Phys.* **92**, 5057 (1990).
- ²⁸C. Jeppesen and K. Kremer, *Eur. Phys. Lett.* **34**, 563 (1996).
- ²⁹J. S. Higgins and H. C. Benoit, *Polymers and Neutron Scattering*, Oxford Series on Neutron Scattering in Condensed Matter (Clarendon Press, 1997).
- ³⁰D. Mukherji, C. M. Marques, T. Stühn, and K. Kremer, "Co-non-solvency as a design principle for smart heteropolymer architectures" (unpublished).
- ³¹P.-G. de Gennes, *Scaling Concepts in Polymer Physics* (Cornell University Press, London, 1979).
- ³²J. Des Cloizeaux and G. Jannink, *Polymers in Solution: Their Modelling and Structure* (Clarendon Press, Oxford, 1990).
- ³³J. G. Kirkwood and F. P. Buff, *J. Chem. Phys.* **19**, 774 (1951).
- ³⁴J. Rösgen, B. M. Pettitt, and D. W. Bolen, *Biophys. J.* **89**, 2988 (2005).
- ³⁵T. L. Hill, *An Introduction to Statistical Thermodynamics* (Courier Dover Publications, 1960).
- ³⁶J. D. Halverson, T. Brandes, O. Lenz, A. Arnold, S. Bevc, V. Starchenko, K. Kremer, T. Stuehn, and D. Reith, *Comput. Phys. Commun.* **184**, 1129 (2013).
- ³⁷W. Humphrey, A. Dalke, and K. Schulten, *J. Mol. Graphics* **14**, 33 (1996).